Journal of Colloid and Interface Science 343 (2010) 109–114

Contents lists available at ScienceDirect

Journal of Colloid and Interface Science

www.elsevier.com/locate/jcis

Hierarchically imprinted polymer substrates for enhanced attachment of *Escherichia coli*

Fengxiang Zhang, Hongzhe Li, Xin Wang, Hong Yee Low *, Xu Li *

*Institute of Materials Research and Engineering, A*STAR (Agency for Science, Technology and Research), 3 Research Link, Singapore 117602, Singapore*

ARTICLE INFO

Article history:
Received 13 August 2009
Accepted 18 November 2009
Available online 24 November 2009

Keywords:
Hierarchical structure
Attachment
Escherichia coli
Enhanced

ABSTRACT

Escherichia coli (*E. coli*) detection is important for ensuring human health and public security. One critical step in most detection methods is to have the *E. coli* cells attach to the substrate or transducer of a biosensor before they can be detected and/or identified. In this context, a chemical or physical enhancement effect arising from the substrate will help to achieve a high sensitivity of bacterial detection. This work makes use of hierarchically imprinted surface structures to demonstrate such effect using quartz crystal microbalance (QCM). Specifically, hierarchical structures are imprinted on polystyrene coated resonance crystals of QCM; such crystals, after incubation in an *E. coli* suspension of reduced concentration (1×10^4 colony forming units/mL), exhibit improved resonance frequency shifts, which are 1–2 orders of magnitude higher than those without the hierarchical structures. The enhancement effect is attributed to the enlarged surface area of the substrate and the way it immobilizes the bacteria. As revealed by scanning electron microscopy, the hierarchical substrates immobilize the *E. coli* cells by both trapping them in the micro-trenches and having them adhere to the nano-protrusions, while the single-level imprinted structures accommodate the cells mainly in the trenches or over the protrusions, instead of both.

1. Introduction

Escherichia coli (*E. coli*) are Gram-negative, pathogenic bacteria that can cause various diseases such as urinary tract infections, inflammations and peritonitis. These diseases are often correlated with direct or indirect pollution of drinking water and food products by *E. coli* Therefore, monitoring and detection of this bacterium in water and food is important for ensuring public health. *E. coli* detection can be achieved through a number of methods such as culture and colony counting [1], polymerase chain reaction [2,3], and different sensing devices including quartz crystal microbalance (QCM) [4,5], electrochemical sensors [6–8], acoustic wave sensors [9,10], and optical biosensors based on surface plasmon resonance [11,12], quantum dots [13,14] and conjugated polymer [15–17].

In a typical process of *E. coli* detection using QCM, the bacteria are first separated and pre-concentrated from a sample of drinking water or milk (1–10 colony forming units per 100 mL, or CFU/mL). After being enriched to a higher concentration (normally above 10^6 CFU/mL), the bacteria suspension is injected into the sample cell of a QCM whose resonator crystal has been surface treated with an antibody. Once the bacteria bind to the resonator surface through the antibody, a shift in the resonance frequency of QCM will be observed, and this is referred to as in situ measurement. Alternatively, one can also adopt an ex situ route, i.e. to measure the frequency of the bare QCM crystal, incubate it in the bacterial suspension, measure the frequency again after incubation and drying, and then make a comparison between the two frequencies. In both cases, bacterial affinity of the QCM crystal will influence the resulting frequency shifts. A poor affinity may result in an insignificant frequency shift that is hardly distinguishable from control or noise, since factors other than mass adsorption, including variation of surface viscoelasticity and solution density and viscosity can all result in a frequency change of the quartz crystal [18]. With these considerations, an effective strategy to improve the bacterial affinity of a biosensor substrate, or to enhance bacterial attachment to the substrate, is necessary for detection of bacteria with a high sensitivity.

Attachment of cells, either eukaryotes or prokaryotes (including *E. coli*), to a substrate like the QCM crystal involves both chemical and physical interactions between the cell and the substrate. Currently, most bacterial attachment is achieved by the use of antibodies, avidins or peptides, which are adsorbed or grafted on surface-functionalized substrates or transducers [19–21,9]. For the purpose of enhancing *E. coli* attachment, combined immbolization of avidin and biotinylated antibody has been adopted on a polyurethane film, which resulted in 5-fold increase in the number of *E. coli* attached in comparison with the blank polyurethane [22]. While topographical features of a substrate surface have been reported to influence attachment or immobilization of eukaryote

* Corresponding authors.
E-mail addresses: hy-low@imre.a-star.edu.sg (H.Y. Low), x-li@imre.a-star.edu.sg (X. Li).

0021-9797/$ - see front matter © 2009 Elsevier Inc. All rights reserved.
doi:10.1016/j.jcis.2009.11.038

cells and some bacterial species [23–25], there is rather limited work on attachment and/or detection of *E. coli* using patterned substrates. The present work will explore this aspect, and investigate the role of surface patterns in *E. coli* attachment to a biosensor substrate. Previously, we have reported a sequential nanoimprinting technique for fabrication of three-dimensional complex structures on different polymer surfaces and the applications of such structures in surface wettability tailoring [26–28]. In this work, we make use of the sequentially imprinted structures to achieve enhanced attachment of *E. coli* to polystyrene substrates. When the hierarchical structures are incorporated on the QCM crystals, the mass of bacteria immobilized is improved by 1–2 orders of magnitude as compared with the case where there is no hierarchical structure on the crystal. We also analyzed the way of *E. coli* attachment on different substrates (with or without hierarchical structures) with the aid of scanning electron microscopy (SEM).

2. Experiments

2.1. Polystyrene imprinting

Polystyrene (PS, Mw = 45,000 g/mol) films were prepared by spin coating on well cleaned, oxygen-plasma-treated glass slides, followed by baking at 150 °C for 5–10 min; the resultant films were about 2.2 μm in thickness. Two types of silicon molds (supplied by Institute of Microelectronics Singapore) were used for imprinting: 2 μm grating (1:1 duty cycle, 2 μm depth) and 250 nm grating (1:1 duty cycle, 250 nm depth). Prior to imprinting, the molds were ultrasonicated in isopropyl alcohol (IPA, 90–100%), rinsed with IPA, treated with oxygen plasma (10 sccm, 100 W, 250 m Torr for 10 min) and subsequently treated with perfluorodecyltrichlorosilane (FDTS, 96%) vapor in a desiccator under reduced pressure. Such treated molds then underwent one dummy imprinting on polycarbonate films (160 °C, 40 bar for 5 min) to get rid of any residual physisorbed FDTS molecules so that these molecules will not transfer to PS surface during imprinting and affect the subsequent bacteria experiment. Imprinting of single-level 2 μm and 250 nm gratings were carried out at 130 °C, 40 bar for 5 min. The hierarchical patterns were obtained by imprinting of 250 nm gratings at 60 °C, 30 bar for 10 min on the pre-imprinted 2 μm gratings with different alignments.

2.2. Bacteria culture and attachment

E. coli strain *DH5-α* was cultured aerobically in Luria Bertani (LB) broth overnight at 37 °C. The glass-supported, imprinted PS films were sterilized by UV irradiation for 15 min before use. Bacterial attachment experiments were performed by impregnating different PS films with the *E. coli* cultures (1×10^4 colony forming units/mL, CFU/mL) in a rocking incubator (rocking speed 100 rpm) and kept at 37 °C. The use of rocking incubator prevented sedimentation of the bacteria over time. After incubation for 4 h, the films were taken out, rinsed rigorously and copiously with phosphate buffered saline (PBS), and dried with nitrogen. The *E. coli* cells on the films were then stained by a combination dye (LIVE/DEAD *Bac*light bacteria viability kits, Molecular Probes, L13152) for fluorescence study.

2.3. Quartz crystal microbalance (QCM) study

QCM studies were performed using a MAXTEK PM 710 Plating Monitor coupled with a MPS-550 Sensor probe. The MAXTEK quartz resonators were made from AT-cut quartz crystals covered by evaporated gold on both faces. The resonators have a 5 MHz resonance frequency and a surface area of 0.316 cm^2. They were spin coated with PS films, which were subsequently imprinted with different grating patterns. In the next step, the resonators, which carry imprinted surface coatings, underwent bacterial attachment following the same procedure as that for glass-supported PS. The QCM frequencies of each resonator with nanoimprinted patterns were measured (5–10 min for frequency stabilization) before and after *E. coli* immobilization.

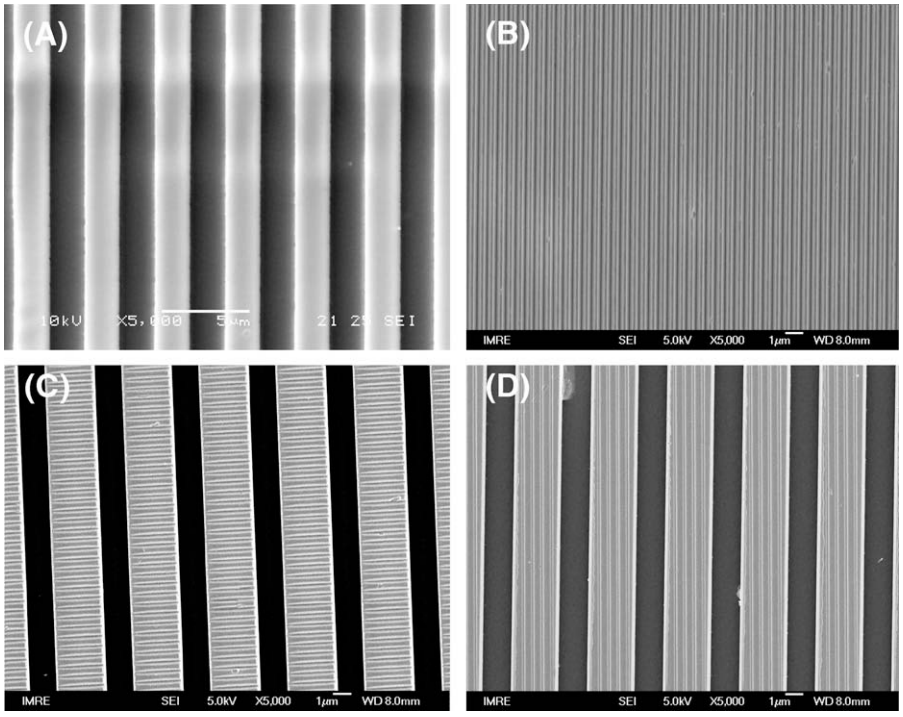

Fig. 1. Surface patterns created on the PS film by nanoimprinting: (A) 2 μm grating, (B) 250 nm grating, (C) 250 nm on 2 μm grating with perpendicular alignment (or 2 μm ⊥ 250 nm), (D) 250 nm on 2 μm grating with parallel alignment (or 2 μm ∥ 250 nm).

2.4. Fluorescence and scanning electron microscopy (SEM) study

The bacteria-carrying samples were stained using a combination dye (LIVE/DEAD *Bac*light bacteria viability kits, Molecular Probes, L13152) and analyzed by a Leica DMLM microscope with a 100 W Hg lamp. SEM images were obtained on a JEOL FEG SEM (JSM6700F). For SEM analysis, all samples were deposited with a thin layer of gold prior to loading into the SEM chamber.

3. Results and discussion

Four types of surface patterns were imprinted on polystyrene (PS) thin films, including single-level 2 μm and 250 nm gratings, and hierarchical patterns consisting of 250 nm grating on 2 μm grating with perpendicular and parallel alignments (denoted as 2 μm ⊥ 250 nm and 2 μm ∥ 250 nm, respectively) between the nano- and micro-features. The single-level patterns were imprinted using the conventional nanoimprint lithography, i.e. imprinting above the glass transition temperature (*Tg*) of the polymer. The hierarchical patterns were made with our previously reported sequential imprinting technique, which involves a primary imprinting above T_g and a subsequent secondary imprint below T_g. All the patterns are uniform, covering large area and almost defect-free as shown in the SEM images (Fig. 1).

The above imprinted PS films were used as substrates for attachment or immobilization of *E. coli DH5-α* from a 1×10^4 CFU/mL suspension. Immobilization was achieved by incubating the imprinted samples in the bacteria suspension at 37 °C for 4 h. The reason for which we chose 1×10^4 CFU/mL bacterial suspension for incubation is that the *E. coli* growth is still in the lag-phase at this concentration, which means the growth rate is quite low; therefore, 4 h incubation may not result in the exponential proliferation at the endpoint of incubation. More importantly, we used a low rocking speed (100 rpm) during incubation. Normally, the speed should be 220–250 rpm. With a lower rocking speed, the growth rate was also reduced. The bacterial concentration at the end point of incubation was ca. 4×10^4 mL^{-1}, which is not too far from the initial level.

Fig. 2 shows the fluorescence images of the different PS films after the *E. coli* immobilization experiments. The presence of bacteria (stained) on these samples was viewed with green and red filters to differentiate between live and dead cells. As can be seen from Fig. 2, both live and dead bacteria have been attached to the substrate surfaces; meanwhile, the surfaces with different patterns exhibited very different affinities toward the bacterial cells. The bare film exhibited only a few bacteria, while the single-level imprinted (2 μm grating and 250 nm grating) samples exhibited slightly more. In contrast, the hierarchically imprinted samples at-

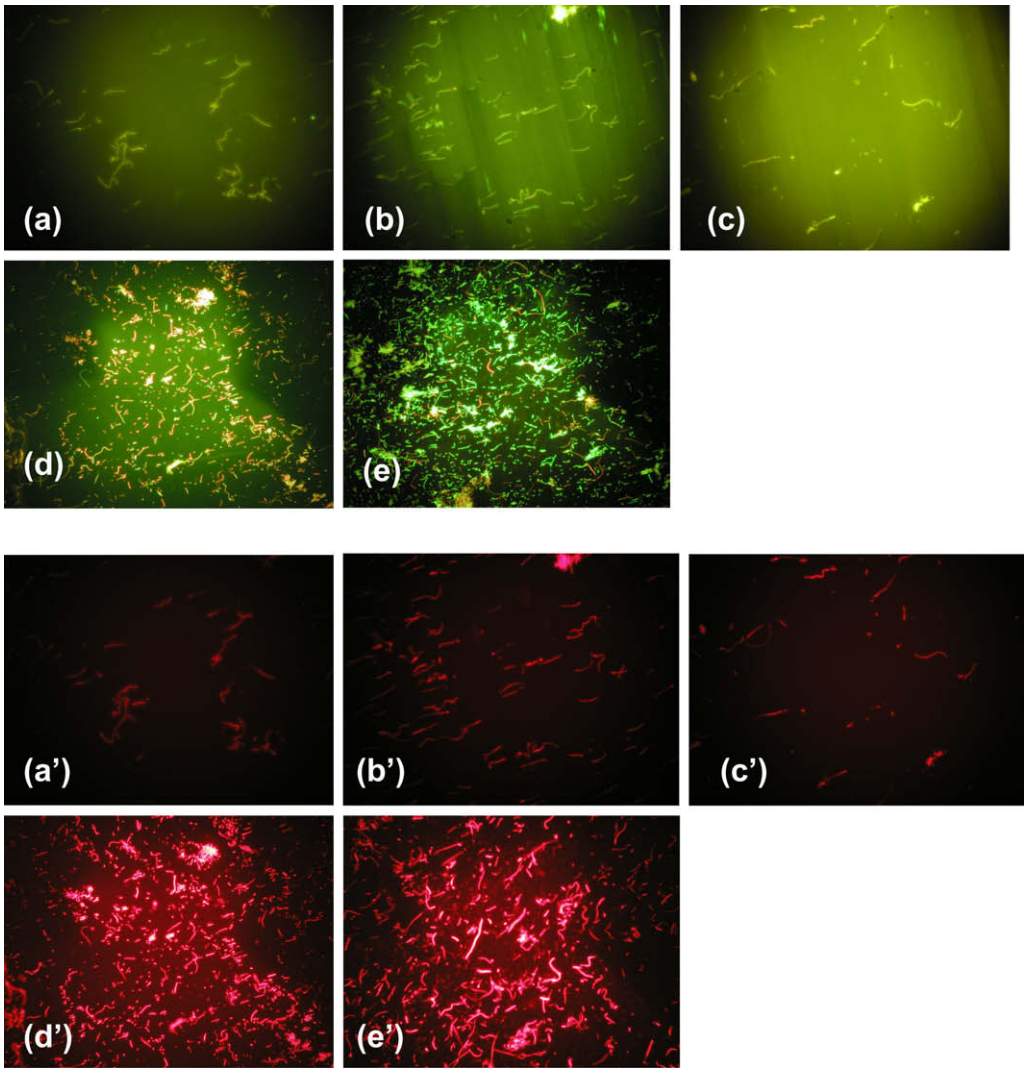

Fig. 2. Fluorescence microscopy images of *E. coli* cells immobilized on different PS films: (a, a′) bare surface, (b, b′) 2 μm grating, (c, c′) 250 nm grating, (d, d′) 250 nm on 2 μm grating with perpendicular alignment (or 2 μm ⊥ 250 nm), (e, e′) 250 nm on 2 μm grating with parallel alignment (or 2 μm ∥ 250 nm). Magnification: 20.

tracted densely populated bacteria (Fig. 2d, e, d′ and e′). Here, it is worthwhile to note that a lot of literature reported *E. coli* concentration of 10^6–10^{10} CFU/mL in different detection methods [29,30]; below this range, the amount of *E. coli* detected or captured is low and the sensing signal is not significant. For example, less than 20 bacteria were seen within a fluorescence image when *E. coli* were detected from a 10^5 CFU/mL sample by the use of nanoparticles [31]. The above result is low in comparison with ours, where we used a lower *E. coli* concentration (1×10^4 CFU/mL) but observed hundreds of *E. coli* colonies immobilized on the hierarchically imprinted surfaces as shown by the fluorescence images (Fig. 2d, e, d′ and e′). Our results clearly demonstrate the substrate surface enhancement effect for *E. coli* attachment, which is attributed to the hierarchical polymer structures on the substrates.

The surface enhancement effect was further investigated and demonstrated using quartz crystal microbalance (QCM). We first coated QCM crystals with PS and made different imprints on the PS coatings as shown in Fig. 1. Resonance frequencies of each coated crystal were measured, and the coated crystals were then incubated in 1×10^4 CFU/mL *E. coli* suspension for 4 h. After incubation, the crystals were rinsed rigorously with phosphate buffer saline and dried with nitrogen; the frequency of each crystal was measured again and compared with that before incubation, and the frequency shifts are shown in Fig. 3. For all samples, a decrease in the frequency was observed, indicating a certain mass of bacteria may have been immobilized on them. However, the frequency decreases are markedly different, and the most significant decreases are seen on the samples with hierarchical patterns; such patterns show frequency shifts of around 1100 Hz, which are 1–2 orders of magnitude larger than those for the bare or single-level imprinted samples. We also carried out a control experiment to look into the effect of culture medium (LB) on the above QCM results, and got a frequency drop of 180 Hz for the QCM crystal carrying 2 μm ⊥ 250 nm pattern and incubated in pure LB for 4 h. This frequency drop is negligibly small in comparison with that resulting from the hierarchical samples, and indicates that the culture medium has negligible influence on the frequency changes.

In QCM bacterial sensors reported in the literature, *E. coli* concentrations of above 1×10^5 CFU/mL are typically used as the starting concentration before the sensor crystal is incubated (as in the ex situ route), or before the solution is injected in the flow module (as in the in situ route). For example, concentration values of 3×10^5–1×10^9 cells/mL, 1×10^6 CFU/mL, and 2.4×10^7 CFU/mL have been reported in Refs. [32–34], respectively. The *E. coli* concentration used in our work (1×10^4 CFU/mL) is low compared with the above values, indicating a lower detection limit. There are also reports where starting concentrations of *E. coli* below 1×10^5 CFU/mL were used (for example 7.5×10^2 cells/mL), but more complex techniques such as carbohydrate and lectin recognition were involved [35]. Here in our work, the surface hierarchical patterning constitutes a new alternative to the reported methods to achieve lower detection limit.

To provide a more tangible comparison among the different sensors' immobilization capacities, we converted the above QCM frequency decreases into mass of adsorbed bacteria by using Sauerbrey equation [4], which is simplified to the following format by taking into account the resonator characteristics: $\Delta m = -17.6 \times A \times \Delta f$, where Δm stands for the mass of immobilization, A is the surface area of the QCM resonator electrode and Δf the frequency shift. The calculated results are shown in Fig. 4, where one can see an *E. coli* mass load of about 20 μg/cm^2 on the 2 μm ⊥ 250 nm patterned surface, which is ca. 2 and 4 times that on 2 μm and 250 nm patterns respectively. It should be mentioned that the above calculation is only a rough estimation of the immobilized bacteria amount, because Sauerbrey equation is valid only when the adsorbed layer is rigid and homogeneous.

There are many reports in the literature on detection of *E. coli* and other bacteria using QCM biosensors. For example, in mannose receptor immobilized QCM sensor the frequency shift was 230 Hz after 2 h incubation in 7.5×10^7 cells/mL solution [35]. Mao et al. [36] developed a nanoparticle amplification based QCM sensor for detection of *E. coli*, and reported a detection signal of about 30 Hz for bacteria sample of 2.67×10^8 CFU/mL. In another report [37], QCM with antibody immobilized resonator surface demonstrated a frequency shift of ca. 350 upon binding of *E. coli*. For other bacteria, Su and Li reported a QCM frequency drop of about 20 Hz in detection of *Salmonella* at a concentration of 10^8 cells/mL [19]. Fung and Wong [38] reported frequency shift of 35 Hz after 50 min of injection of 1.7×10^4 cells/mL of *Solmonella paratyphi A.* into QCM flow cell. Compared with the above methods and results for bacteria sensing, where no sensor surface effect came into play, our QCM sensor with hierarchically imprinted surface coating clearly showed stronger detection signal at relatively low bacteria concentration, meaning that the sensitivity is improved. This is the advantage of our method. However, we did not use antibody modification for the sensor surface, so non-specific binding does exist. In our future work, efforts will be made to introduce antibody onto the hierarchical surface so that enhanced, highly specific binding and detection of *E. coli* might be achieved.

In order to find out how the enhancement effect comes into being, we performed a scanning electronic microscopy (SEM) study. Fig. 5 shows the SEM images of immobilized *E. coli* on the

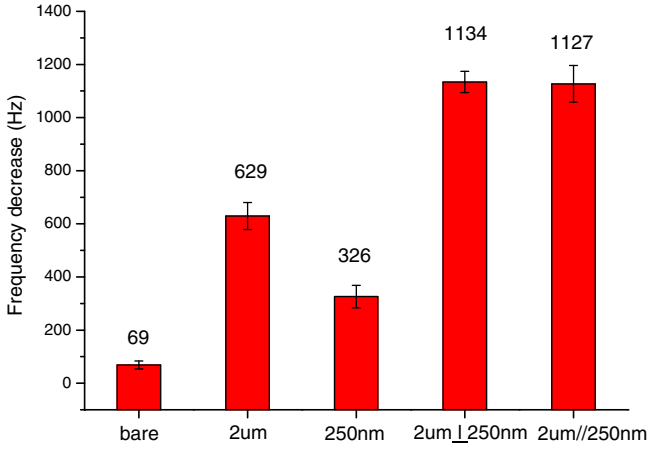

Fig. 3. QCM frequency shifts upon *E. coli* immobilization on different patterned PS surfaces.

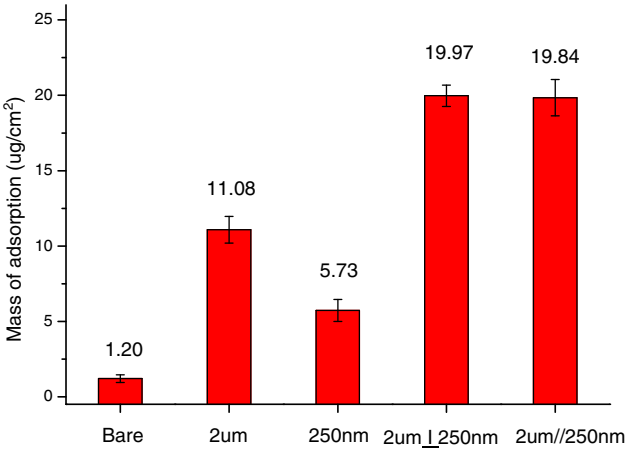

Fig. 4. Masses of *E. coli* immobilized on different patterned PS surfaces.

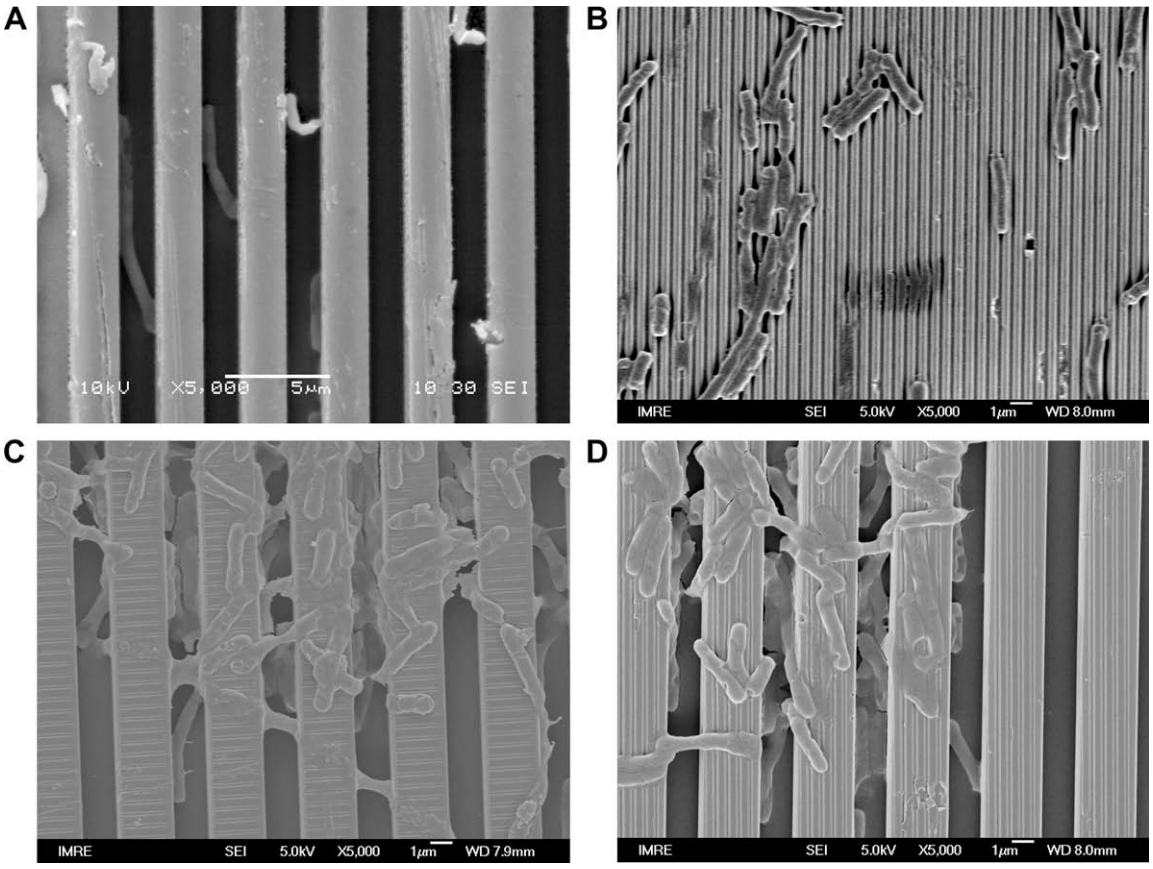

Fig. 5. SEM images of *E. coli* on (A) 2 μm grating, (B) 250 nm grating, (C) 250 nm on 2 μm grating with perpendicular alignment (or 2 μm ⊥ 250 nm), (D) 250 nm on 2 μm grating with parallel alignment (or 2 μm ∥ 250 nm) PS surfaces.

imprinted PS surfaces. It is seen that *E. coli* formed large aggregates on the hierarchical patterns, while they deposited sparsely or with smaller aggregates on the 2 μm grating and 250 nm grating patterns. According to the SEM images, the *E. coli* cells have a lateral dimension of ca. 500 nm. With this dimension compared to that of the substrate patterns, the cells will preferably attach to 2 μm grating by getting trapped in the trenches, and attach to 250 nm grating by lying across or hanging over the protrusions. The above two ways of bacterial attachment occur simultaneously on the hierarchical patterns, i.e., the bacteria can both be trapped inside the micro-trenches, and also adhere to the nano-protrusions. This "trapping plus adherence" mechanism helps to explain why the hierarchically imprinted surface showed greatly enhanced immobilization of bacteria molecules. Meanwhile, it is known that the bacterial membrane surface has filamentous appendages such as flagella, fimbriae and pili, which can help the bacterial creature to adhere to or grasp a surface. Such adhesion or grasping force will become stronger when the bacteria's filamentous appendages get in touch with the complex surface features on the hierarchical patterns because of the increased contact area, so that the bacteria firmly attach to the patterns and can withstand rigorous rinse after incubation.

4. Summary

We have demonstrated enhanced attachment of *E. coli* cells onto polystyrene substrates. The enhancement was achieved through the use of hierarchical surface structures imprinted on the substrates, which consist of 250 nm grating imprinted on 2 μm grating with various alignments. Fluorescence microscopy and QCM results showed that the substrates with hierarchical structures had significantly larger amount of bacteria attached than those bare or with single-level patterns. On hierarchical patterns, the *E. coli* cells both adhere to the nano-features and also get trapped inside the trenches of the micro-patterns. The resulting substrate enhancement effect, though still lacking data on specific interaction with bacteria, will be beneficial for improving the detection sensitivity of biosensors for bacteria.

References

[1] A. Singh, B.H. Pyle, G.A. McFeters, J. Microbiol. Meth. 10 (1989) 91–101.
[2] C. Bischoff, J. Lqthy, M. Altwegg, F. Baggi, J. Microbiol. Meth. 61 (2005) 335–341.
[3] S. Sandhya, W. Chen, A. Mulchandani, Anal. Chim. Acta 614 (2008) 208–212.
[4] Z. Shen, M. Huang, C. Xiao, Y. Zhang, X. Zeng, P.G. Wang, Anal. Chem. 79 (2007) 2312–2319.
[5] V.C.H. Wu, S.H. Chen, C.S. Lin, Biosens. Bioelectron. 22 (2007) 2967–2975.
[6] Y.H. Lin, Sz-Hau Chen, Yao-Chen Chuang, Yi-Chen Lu, Thomas Y. Shen, C. Allen Chang, Chih-Sheng Lin, Biosens. Bioelectron. 23 (2008) 1832–1837.
[7] C. Ruan, L. Yang, Y. Li, Anal. Chem. 74 (2002) 4814–4820.
[8] P. Geng, X. Zhang, W. Meng, Q. Wang, W. Zhang, L. Jin, Z. Feng, Z. Wu, Electrochim. Acta 53 (2008) 4663–4668.
[9] N. Moll, E. Pascal, D.H. Dinh, J.P. Pillot, B. Bennetau, D. Rebiere, D. Moynet, Y. Mas, D. Mossalay, J. Pistŕe, C. Ďejous, Biosens. Bioelectron. 22 (2007) 2145–2150.
[10] E. Berkenpas, P. Millard, M. Pereira Da Cunha, Biosens. Bioelectron. 21 (2006) 2255–2262.
[11] A.D. Taylor, J. Ladd, Q. Yu, S. Chen, J. Homola, S. Jiang, Biosens. Bioelectron. 22 (2006) 752–758.
[12] A. Subramanian, J. Irudayaraj, T. Ryan, Biosens. Bioelectron. 21 (2006) 998–1006.
[13] E. Tully, S. Hearty, P. Leonard, R. O'Kennedy, Int. J. Biol. Macromol. 39 (2006) 127–134.
[14] Y.C. Kuo, Q. Wang, C. Ruengruglikit, H. Yu, Q. Huang, J. Phys. Chem. C 112 (2008) 4818–4824.

[15] Y. Scindia, L. Silbert, R. Volinsky, S. Kolusheva, R. Jelinek, Langmuir 23 (2007) 4682–4687.
[16] Y.L. Su, J. Li, L. Jiang, J. Cao, J. Colloid Interface Sci. 284 (2005) 114–119.
[17] M.G. Baek, R.C. Stevens, D.H. Charych, Bioconjugate Chem. 11 (2000) 777–788.
[18] S.J. Martin, V.E. Granstaff, G.C. Frye, Anal. Chem. 63 (1991) 2272–2281.
[19] X.L. Su, Y. Li, Biosens. Bioelectron. 19 (2004) 563–574.
[20] N.V. Kulagina, M.E. Lassman, F.S. Ligler, C.R. Taitt, Anal. Chem. 77 (2005) 6504–6508.
[21] K.Y. Gfeller, N. Nugaeva, M. Hegner, Biosens. Bioelectron. 21 (2005) 528–533.
[22] R.R. Koepsel, A.J. Russell, Biomacromolecules 4 (2003) 850–855.
[23] K.A. Simon, E.A. Burton, Y. Han, J. Li, A. Huang, Y.Y. Luk, J. Am. Chem. Soc. 129 (2007) 4892–4893.
[24] K.A. Whitehead, J. Verran, Food Bioprod. Process. 84 (C4) (2006) 253–259.
[25] C. Satriano, G.M.L. Messina, S. Carnazza, S. Guglielmino, G. Marletta, Mater. Sci. Eng., C 26 (2006) 942–946.
[26] F. Zhang, H.Y. Low, Nanotechnology 17 (2006) 1884.
[27] F. Zhang, H.Y. Low, Langmuir 23 (2007) 7793.
[28] F. Zhang, J. Chan, H.Y. Low, Appl. Surf. Sci. 254 (2008) 2975.
[29] M. Namura, T. Hijikata, K. Miyanaga, Y. Tanji, Biotechnol. Prog. 24 (2008) 481–486.
[30] Z. Ma, J. Li, L. Jiang, Langmuir 16 (2000) 7801–7804.
[31] K. El-Boubbou, C. Gruden, X. Huang, J. Am. Chem. Soc. 129 (2007) 13392–13393.
[32] C. Poitras, N. Tufenkji, Biosens. Bioelectron. 24 (2009) 2137–2142.
[33] M. Plomer, G.G. Guilbault, B. Hock, Enzyme Microb. Technol. 14 (1992) 230–235.
[34] T. Alava, N. Berthet-Duroure, C. Ayela, E. Trévisiol, M. Pugnière, Y. Morel, P. Rameil, L. Nicua, Sensor Actuat B 138 (2009) 532–538.
[35] G. Sauerbrey, Z. Phys. 155 (1959) 206.
[36] X. Mao, L. Yang, X.L. Su, Y. Li, Biosens. Bioelectron. 21 (2006) 1178–1185.
[37] N. Adányi, M. Váradi, N. Kim, I. Szendro, Curr. Appl. Phys. 6 (2006) 279–286.
[38] Y.S. Fung, Y.Y. Wong, Anal. Chem. 73 (2001) 5302–5309.